Title
Protein dynamics. Comparative investigation on heme-proteins with different physiological roles

Journal
Biophysical Journal, 59(3)

ISSN
0006-3495

Authors
Di Iorio, EE
Hiltpold, UR
Filipovic, D
et al.

Publication Date
1991-03-01

DOI
10.1016/s0006-3495(91)82287-1

Protein dynamics

Comparative investigation on heme-proteins with different physiological roles

Ernesto E. Di Iorio,* Urs R. Hiltpold,* Dorde Filipovic,* Kaspar H. Winterhalter,* Enrico Gratton,‡ Eugenio Vitrano,§ Antonio Cupane,§ Maurizio Leone,§ and Lorenzo Cordone§

*Laboratorium für Biochemie I, Eidgenössische Technische Hochschule 8092 Zurich, Switzerland; ‡Department of Physics, University of Illinois at Urbana-Champaign, Urbana, IL 61801 USA; and §Istituto di Fisica and GNSM-CISM, 90123, Palermo, Italy

ABSTRACT We report the low temperature carbon monoxide recombination kinetics after photolysis and the temperature dependence of the visible absorption spectra of the isolated α^{SH}-CO and β^{SH}-CO subunits from human hemoglobin A in ethylene glycol/water and in glycerol/water mixtures. Kinetic measurements on sperm whale (*Physeter catodon*) myoglobin and previously published optical spectroscopy data on the latter protein and on human hemoglobin A, in both solvents, (Cordone, L., A. Cupane, M. Leone, E. Vitrano, and D. Bulone. 1988. *J. Mol. Biol.* 199:312–218) are taken as reference.

Low temperature flash photolysis data are analyzed within the multiple substates model proposed by Frauenfelder and co-workers (Austin, R. H., K. W. Beeson, L. Eisenstein, H. Frauenfelder, and I. C. Gunsalus. 1975. *Biochemistry.* 14:5355–5373). Within this model a distribution of activation enthalpies for ligand binding accounts for the structural heterogeneity of the protein, while the preexponential factor, containing also the entropic contribution to the free energy of the process, is considered to be constant for all conformational substates. Optical spectra are deconvoluted in gaussian components and the temperature dependence of the moments of the resulting bands is analyzed, within the harmonic Frank–Condon approximation, to obtain information on the stereodynamic properties of the heme pocket. The kinetic and spectral parameters thus obtained are found to be protein dependent also with respect to their sensitivity to changes in the composition of the external medium. A close correlation between the kinetic and spectral features is observed for the proteins examined under all experimental conditions studied. The results reported are discussed in terms of differences in the heme pocket structure and in the conformational heterogeneity among the various proteins, as related to their different capability to accommodate constraints imposed by the external medium.

INTRODUCTION

It is generally accepted that structural fluctuations are necessary for the penetration of ligands or substrates from the solvent to the active site, through the protein matrix. However, a regulatory role of protein dynamics at the functional level is still often questioned. To gain insights into this matter, we started a comparative study on the dynamic properties of proteins with different physiological roles, i.e., myoglobins on one side and hemoglobin or its isolated subunits on the other, using optical spectroscopy and flash photolysis as experimental approaches.

The temperature dependence of optical absorption spectra of heme proteins can be related to the interactions of the optical electrons with nuclear vibrations (Cordone et al., 1986, 1988; Cupane et al., 1988; Leone et al., 1987; Schomacker and Champion, 1986; Srajer et al., 1986). Based on this correlation, the optical spectra thermal behavior of SW-Mb[1] and Hb-A has been investigated (Cordone et al., 1986, 1988; Cupane et al., 1988; Leone et al., 1987). The temperature dependence (between 20 and 300 K) of the first (M_1) and second (M_2) moment of all observed optical absorption bands of human deoxy, oxy-, and carbonyl-HbA, can be rationalized in terms of a harmonic model for the coupling between the optical electrons and the nearby nuclei (Eq. 2 in Theoretical Background) and is not influenced by the replacement of ethylene glycol with glycerol in the external medium. In contrast, in deoxy, oxy-, and carbonyl-SW-Mb a considerable solvent dependence of M_1 is observed, but not of M_2, and the model fails in predicting the thermal evolution of the first moment while being successful with the second. The different behavior of SW-Mb as compared with Hb was suggested to arise from the different aggregation state of the two

This work is dedicated, with immense admiration and gratitude, to Prof. Jeffries Wyman in occasion of his 90th birthdate.

Dr. Dorde Filipovic's present address in Department of Biochemistry, University of Illinois at Urbana Champaign, 1209 West California Street, Urbana, IL 61801 USA.

[1] *Abbreviations used in this paper:* Hb = hemoglobin; HbA = major human adult hemoglobin; SW-Mb = sperm whale (*Physeter catodon*) myoglobin; PMB = *p*-mercuribenzoate; α^{SH} and β^{SH} = isolated α and β subunits from HbA with free SH groups; α^{PMB} and β^{PMB} = isolated α and β subunits from HbA with the SH groups reacted with PMB; M_0, M_1, and M_2 = zeroth, first and second moments of deconvoluted optical absorption bands related, respectively, to their area, peak position and width.

0006-3495/91/03/742/13 $2.00

proteins and/or from intrinsic structural and dynamic properties of their heme pocket (Cordone et al., 1988).

Flash photolysis as a function of temperature provides information on the effect of dynamics on the functional behavior of proteins (see e.g., Ansari et al., 1986; Austin et al., 1975). This approach has been used in a comparative study on several myoglobins and Hb subunits using glycerol/water as solvent (Winterhalter and Di Iorio, 1987). Systematic differences were observed between the two classes of proteins. The activation enthalpies for CO rebinding from inside the heme pocket, as obtained from low temperature kinetics, are higher in the myoglobins than in the Hb subunits and this situation is reflected in a higher degree of geminate ligand recombination at room temperature in the hemoglobin chains than in the myoglobins. Furthermore, the distribution of activation enthalpies derived from the flash photolysis measurements at cryogenic temperatures (see Eq. 3 in Theoretical Background) is considerably broader for the myoglobins and the β^{SH} Hb subunits than for the α^{SH} chains (Alberding et al., 1978; Winterhalter and Di Iorio, 1987). The same behavior is observed when the chains are inserted in iron-cobalt hybrids (Winterhalter and Di Iorio, 1987), therefore excluding effects of the higher aggregation state of the "free" β^{SH} subunits in determining their larger distribution of enthalpies. These findings were explained in terms of a different deformability of the heme pocket in the various proteins (Winterhalter and Di Iorio, 1987).

Here we combine the efforts of the Palermo and Zurich groups and compare the thermal behavior of both optical spectra and CO recombination kinetics after photolysis of the α^{SH} and β^{SH} human Hb subunits and of SW-Mb in ethylene glycol/water and glycerol/water mixtures.

THEORETICAL BACKGROUND

Optical spectroscopy

Electronic transitions are coupled to the vibrational motion of the nearby nuclei. This coupling explains the sharpening and shift of the optical absorption bands which is observed when the temperature is lowered. A theory on electron-vibration coupling, which accounts for the temperature dependence of the optical spectra of color centers in crystals, has been developed long ago (see e.g., Markham, 1959). The electronic transition from the ground to the excited state is considered to be instantaneous as compared with nuclear motions (Franck–Condon approximation) and the electron-lattice interaction energy to be quadratic in the displacement of the nuclei from their equilibrium positions. According to this theory, which has been successfully applied to study the optical absorption spectra of hemeproteins (Cordone et al., 1986, 1988; Cupane et al., 1988; Leone et al., 1987; Schomacker and Champion, 1986; Srajer et al., 1986), the temperature dependence of the first and second moments of an absorption band is given by:

$$M_1 = \frac{\Delta E}{h} + \frac{2\pi^2}{h}\sum_j S_j R_j \nu_j(g) + \frac{1}{4}\sum_j (R_j - 1)\,\nu_j(g)\coth\frac{h\nu_j(g)}{2kT} \quad (1a)$$

$$M_2 = \frac{2\pi^2}{h}\sum_j S_j R_j^2 \nu_j^2(g)\coth\frac{h\nu_j(g)}{2kT} + I^2, \quad (1b)$$

where k and h are the Boltzmann's and Planck's constants, ΔE is the energy difference between the excited and ground electronic states when the nuclei are at rest in their equilibrium positions, S_j and R_j are the Franck–Condon linear and quadratic coupling constants of the jth normal mode with the electronic transition, and $\nu_j(g)$ is the frequency of the jth normal mode when the electron is in the ground state. It is common practice to neglect the terms containing $(R_j - 1)^2$ in the equation of M_2 (Markham, 1959; Schomacker and Champion, 1986). The sums are extended over the entire set $\{j\}$ of normal modes to which the electronic transition under consideration is coupled. In Eq. 1*b* the term I^2 takes into account the temperature independent homogeneous broadening due to the finite lifetime of the excited state (Schomacker and Champion, 1986). If conformational heterogeneity (structural disorder) is present, the sums in Eqs. 1 must be extended also over all spectrally different species; in this case ΔE is an average value and I^2 takes into account also inhomogeneous broadening due to the presence of spectroscopically different conformational substates. A direct use of Eqs. 1 to evaluate experimental data does not easily yield meaningful information on the various fitting parameters due to their large number. Therefore, the following simplified forms of Eqs. 1, obtained by averaging over all normal modes and conformational species, are widely used (Baldini et al., 1965: Markham, 1959):

$$M_1 = D + F\cdot\coth(h\bar{\nu}/2kT) \quad (2a)$$

$$M_2 = A\cdot\coth(h\bar{\nu}/2kT) + C^2, \quad (2b)$$

where the parameter $\bar{\nu}$ is a "mean effective" frequency of the nuclear motions coupled to the electronic transition. The term C^2 includes I^2 of Eq. 1*a* together with other constant contributions arising from the coupling of the optical electrons with zero-point vibrations of high frequency modes, not populated in the temperature

range investigated. Analogous contributions to M_1 are included in the parameter D. As can be clearly seen from a comparison of Eqs. 1*a* and 2*a* and Eqs. 1*b* and 2*b*, parameters A and F are related respectively to the "mean effective" linear and quadratic terms of the electron-lattice coupling.

The various parameters appearing in Eqs. 2 are considered to be temperature independent. This assumption is tenable only if no relevant structural changes occur when the temperature is lowered. It is worth mentioning that assuming C^2 temperature independent does not mean that the rate of interconversion between substates is not influenced by the temperature, but simply that it is, at all temperatures, much slower than the electronic transitions.

Flash photolysis

At physiological temperatures, the ligand recombination kinetics to monomeric heme proteins is characterized by at least three processes, only one of which has an exponential time dependence and is influenced by the free ligand concentration in the solvent (Austin et al., 1975). The three processes are interpreted in terms of a sequential-barriers model (Ansari et al., 1986; Austin et al., 1975) in which the exponential component is related to the penetration of the ligand from the solvent into the protein (solvent process), the slower of the two nonexponential components is assigned to the migration of the ligand through the protein matrix (matrix process), and the other to its combination to the iron directly from inside the heme pocket (pocket process). Below ~120 K only ligand binding from within the heme pocket is observed; the protein is frozen in many conformational substates whose distribution reflects the dynamic properties of the system at physiological temperatures (Ansari et al., 1986; Dlott et al., 1983; Doster et al., 1982). Within this substates-model the time course for ligand binding at cryogenic temperatures is given by

$$N(t) = \int_0^\infty g(H) \cdot \exp[-k(H, T) \cdot t]\, dH, \qquad (3)$$

where $N(t)$ is the fraction of heme sites which, at time t after photolysis, has not yet rebound a ligand and $g(H)$ is the probability distribution function of finding a protein molecule in a substate characterized by a ligand binding activation enthalpy between H and $H + dH$. The temperature dependence of k in Eq. 3 is assumed to follow Arrhenius' law, i.e.

$$k(H, T) = k_0 \cdot \exp(-H/RT), \qquad (4)$$

where k_0 is the preexponential factor, also containing the entropic contributions to the reaction, and R is the gas constant.

It is difficult to obtain $g(H)$ by numeric inversion of the integral in Eq. 3, being this an ill-conditioned procedure. Instead, it is common practice to use an analytical function to describe the enthalpy distribution and fit the parameters of the function to the experimental data. Several more or less empirical approaches have been used for this purpose (see e.g., Young and Bowne, 1984; Srajer et al., 1988).

MATERIALS AND METHODS

Sperm whale myoglobin

SW-Mb was purchased from Sigma Chemical Co. (St. Louis, MO) and used without further purification.

Hemoglobin chains

Human α^{SH} and β^{SH} hemoglobin subunits were prepared in the CO form after a modification of previously published procedures (Bucci, 1981; Geraci et al., 1969; Ikeda-Saito et al., 1981). For this purpose 25 ml of a freshly prepared Hb solution (~ 1 mM on heme basis) are mixed with 4.25 ml of 0.2 M KH_2PO_4 and 4.25 ml of 2 M KCl. Separately, 50 mg of *p*-chloro-mercuribenzoic acid (Sigma Chemical Co., St. Louis, MO) are dissolved in a minimal volume of 0.1 M KOH and diluted to 10 ml with 20 mM KH_2PO_4. 9 ml of the resulting PMB solution are added to the Hb (PMB/heme ratio ~ 5:1) and, after adjusting the pH to 6 with 2 M KH_2PO_4, the mixture is saturated with CO and incubated at 0°C for 24 h. The small precipitate possibly present is removed by centrifugation at 35,000 × *g* for 10 min and the clear solution is applied on a Sephadex G-25 column (ϕ 3.5 × 60 cm) equilibrated with 7 mM phosphate (obtained by dilution of 1 M phosphate buffer pH 6.8) and eluted with the same buffer. The protein solution is then applied on a Whatman CM-52 column (ϕ 2.5 × 8 cm) also equilibrated with 7 mM phosphate and the β^{PMB} chains are eluted with the same buffer. The column is then washed with 20 mM phosphate (again obtained by dilution of 1 M phosphate buffer pH 6.8) to remove the unsplitted HbA and subsequently the α^{PMB} subunits are eluted as a sharp concentrated band with 0.1 M phosphate buffer pH 7. Immediately after the elution from the CM-52 column the PMB chains are concentrated at 0°C to 15 ml with an ultrafiltration chamber under 300–400 kPa of pure CO. For SH groups regeneration a Sephadex G-25 column (ϕ 3.5 × 60 cm) is equilibrated with 0.1 M Tris-HCl buffer pH 7.4 containing 0.1 M KCl and 0.5 mM EDTA. 15 ml of the equilibration buffer containing 10 mM 2-mercaptoethanol are applied on the G-25 column immediately followed by the 15 ml of PMB chains. The subunits with regenerated SH groups are eluted with 2-mercaptoethanol free buffer. After a solvent exchange to 10 mM phosphate pH 7 and a concentration, by ultrafiltration under CO, to ~10 mM the subunits are checked for purity and complete SH groups regeneration by isoelectric focusing and UV absorption spectroscopy (Winterhalter and Colosimo, 1971). The concentrated stock solutions of α^{SH}-CO and β^{SH}-CO chains are stored in liquid nitrogen in small aliquots to be thawed only immediately before use.

Sample preparation

All samples were prepared by diluting concentrated protein stocks solutions into water-cosolvent-buffer mixtures previously equilibrated with CO and containing 65% (vol/vol) glycerol or ethylene glycol in water and 0.1 M phosphate buffer (pH 7 in water at room temperature); $\sim 3 \cdot 10^{-4}$ M sodium dithionite was also added anaerobically. Final protein concentrations were of the order of 10^{-4} M. 65% cosolvent concentration was chosen to allow the comparison of the spectroscopic data on the isolated Hb subunits with those on SW-Mb and Hb published previously (Cordone et al., 1988). For the spectrophotometric measurements the samples were transferred anaerobically to a 1-cm metacrylate cell (UV grade; Kartell, Italy) as previously described (Cordone et al., 1986). Samples for flash photolysis were anaerobically transferred to a gold-plated copper cell with a 1.2-mm optical path and equipped with metacrylate windows. The use of metacrylate is a necessary prerequisite to obtain perfectly transparent samples over the entire temperature range investigated; as already reported by Cordone et al. (1986), no effect of temperature on the baseline could be detected in the 400–800-nm region when the solvent-cosolvent mixture was measured. Glycerol (Carlo Erba, Milan, Italy, or Fluka, Buchs, Switzerland) and ethylene glycol (Fluka) were analytical grade and used without further purification.

Instrumentation

For the flash photolysis measurements a Nd:YAG pulsed laser (YG471 A/P; Quantel, Orsay, France) was used as photolyzing source. This laser is capable of delivering 12-ns light pulses with an energy of up to 400 mJ at 532 nm. Typically, 70-mJ pulses were used. The sample was kept at the desired temperature using a continuous flow CF 100 cryostat equipped with a temperature controller (Oxford, Osney Mead, Oxford, UK). Monitoring of the CO recombination after photolysis was done at 436 nm and data were simultaneously collected on a 100-MHz 8 bit linear waveform recording system (TR8018 and MM8103A; Le Croy, Chestnut Ridge, NY) and a 1-MHz 12 bit transient recorder with logarithmic data averaging (Wondertoy II, Department of Physics of the University of Illinois at Urbana-Champaign). Measurements were performed from 40 to 110 K every 10 K and after each flash the sample was heated up to 140 K to allow complete relaxation. For each temperature three to five measurements were mediated and the resulting trace was logarithmically time averaged to give a total of 15–40 data-points (transmittance with standard deviation vs. time).

The experimental setup and methods for the optical measurements have been described previously (Cordone et al., 1986; Leone et al., 1987). The spectra were taken on a Jasco Uvidec 650 spectrophotometer; the spectral bandwidth was fixed to 0.4 nm and the time constant to 1 s. Data were recorded at 0.4-nm intervals on magnetic tape for later analysis. To allow comparison of the presently reported spectra with those of HbA-CO and Mb-CO, previously obtained on a Cary 118C spectrophotometer (Cordone et al., 1988), the wavelength calibration of the two instruments was carefully checked by scanning the 586 nm emission line of a deuterium lamp.

Data analysis

Flash photolysis traces were analyzed by global least squares fitting to Eqs. 3 and 4 or, when needed, to a sum of two distributed processes of the type

$$N(t) = f \int_0^\infty g_1(H) \cdot \exp[-k_1(H, T) \cdot t]\, dH + (1 - f) \int_0^\infty g_2(H) \cdot \exp[-k_2(H, T) \cdot t]\, dH. \quad (5)$$

For the enthalpy distributions the modified Γ function

$$g(H) = H^{3\mu-1} \exp(-\Psi \cdot H) \quad (6)$$

was used, where the enthalpy peak position is given by

$$H_{peak} = (3\mu - 1)/\Psi. \quad (7)$$

A large value of Ψ corresponds to a narrow distribution width. The integral in Eq. 5 was computed numerically by the Romberg method to an accuracy of 10^{-5} ΔOD units per each value of time and the total area of the enthalpy distribution was normalized to unity. The global reduced χ^2 was minimized according to Marquardt (Marquardt, 1963) in the ΔOD space, weighting each experimental point on the basis of its reciprocal variance computed from the standard deviation in transmittance (Bevington, 1969). After convergence was reached the χ^2 surface around the minimum was analyzed with respect to each fitting parameter and the 67% confidence limits were thus estimated (resulting in nonsymmetric errors) along with the correlations between parameters (Beechem and Gratton, 1988). Both fitting procedures and error analysis of the fitted parameters were done on IBM compatible personal computers.

The spectral deconvolution in terms of gaussian components $G(\nu) = A \cdot \exp[-(\nu - \nu_0)^2/2\sigma^2]$ was performed on a HP-1000 computer. The mean square deviation was minimized using a nonlinear least-squares algorithm. The zeroth, first, and second moment of each band were calculated according to

$$M_0 = \int_0^\infty \epsilon(\nu)\, d\nu \quad (8a)$$

$$M_1 = \int_0^\infty \frac{\nu \cdot \epsilon(\nu)}{M_0}\, d\nu \quad (8b)$$

$$M_2 = \int_0^\infty \frac{\nu^2 \cdot \epsilon(\nu)}{M_0}\, d\nu - M_1^2, \quad (8c)$$

where $\epsilon(\nu)$ is the absorbance at the optical frequency ν of the relevant gaussian component. Within the so called narrow band approximation (Dexter, 1958), M_0 is proportional to the oscillator strength and Eqs. 8*b*, *c* are the first and second spectral moments which satisfy Eqs. 2*a*, *b*, respectively. To fit the Q_0 band, assigned to a $\pi \rightarrow \pi^*$ transition (Eaton et al., 1978; Eaton and Hofrichter 1981), two gaussians are needed over the entire temperature range (see also Cordone et al., 1986). Therefore, the moments relative to Q_0 are calculated from the distributions resulting from the sum of G_1 and G_2. The Q_v band, interpreted as a vibronic of Q_0 (Eaton et al., 1978; Eaton and Hofrichter, 1981), is well approximated by a single gaussian. We analyze the moments of Q_0 and Q_v, rather than those of the individual gaussians, because G_1 and G_2 are not assigned to particular electronic transitions.

RESULTS

As an example of our kinetic data and of the results of our fitting procedures we report in Fig. 1 the time

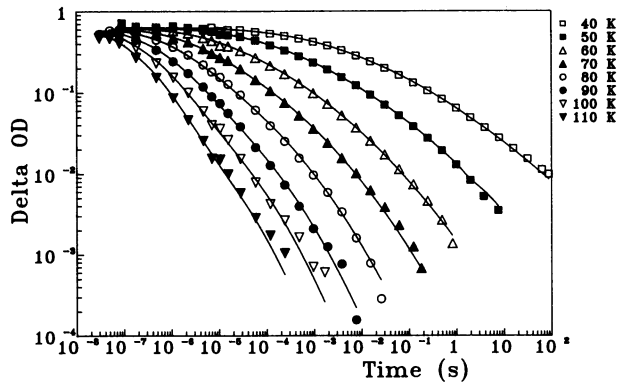

FIGURE 1 CO rebinding time courses after photolysis to the isolated α^{SH} chains from human Hb, in 65% ethylene glycol/water containing 0.1 M phosphate pH 7 in water at 293 K, measured between 40 and 110 K. Together with the experimental data the fitted curves, corresponding to the parameters given in Table 1, are also drawn as continuous lines. The global reduced χ^2 value for the fit is 4.034.

courses relative to CO rebinding to the α^{SH} chains in ethylene glycol between 40 and 110 K, together with the fitted curves corresponding to the parameters given in Table 1. The effect of the solvent composition on the CO rebinding kinetics of the investigated proteins at 60 and 100 K are depicted in Fig. 2. Sizable differences between the time courses in the two solvents are seen for the β^{SH} while for the α^{SH} chains and SW-Mb small changes in the kinetic behavior in the two solvents are observed (note the logarithmic scale). It should also be noted that, while the CO recombination to SW-Mb after photolysis is faster in glycerol than in ethylene glycol, the opposite is true for the Hb chains.

Fig. 3 shows the distributions of activation enthalpies for CO binding from inside the heme pocket relative to the α^{SH} and β^{SH} subunits and to SW-Mb, both in 65% ethylene glycol and glycerol. The relative values of the fitting parameters are given in Table 1. It should be noted that for the α^{SH} and β^{SH} chains, in both solvents, the sum of two Γ functions (Eqs. 4 and 5), with temperature-dependent amplitudes (Table 2), is needed to fit the data while a single distribution (Eqs. 3 and 4) satisfactorily fits the SW-Mb kinetics. The second distribution needed to fit the CO recombination to the Hb chains has, at all temperatures, a small amplitude compared with the total (Table 2). Furthermore, the χ^2 values obtained when the parameters relative to the two enthalpy distributions are left independently free during

TABLE 1 Fitting parameters relative to CO binding kinetics between 40 and 110 K to the α^{SH} and β^{SH} Hb subunits and to SW-Mb in 65% glycerol and 65% ethylene glycol. 67% confidence limits are given in square brackets

	α chains				β chains			
	Glycerol		Eth. glyc.		Glycerol		Eth. glyc.	
Comp. 1								
μ	5.93	[6.45 5.21]	6.91	[7.06 6.61]	2.09	[2.35 1.89]	3.79	[4.19 3.25]
Ψ (*mol/kJ*)	3.05	[3.30 2.75]	3.76	[3.86 3.55]	1.14	[1.26 1.08]	2.63	[2.78 2.42]
H_{peak} (*kJ/mol*)	5.51		5.25		4.62		3.95	
Log k_0/s^{-1}	9.18	[9.29 9.07]	9.23	[9.30 9.18]	9.63	[9.74 9.52]	8.68	[8.99 8.39]
Comp. 2								
Log k_0/s^{-1}	6.91	[7.14 6.76]	7.37	[7.53 7.05]	5.56	[6.03 5.13]	6.16	[6.50 5.85]

	Sperm whale Myoglobin			
	Glycerol		Eth. glyc.	
μ	3.51	[3.86 3.22]	2.80	[3.32 2.70]
Ψ (*mol/kJ*)	0.90	[0.99 0.83]	0.74	[0.81 0.68]
H_{peak} (*kJ/mol*)	10.59		10.00	
Log k_0/s^{-1}	9.01	[9.33 8.81]	7.82	[8.02 7.57]

H_{peak} is not a fitting parameter and is computed from μ and Ψ according to Eq. 7. All samples contain 0.1 M phosphate pH 7 in water at 293 K. More details are given under Materials and Methods.

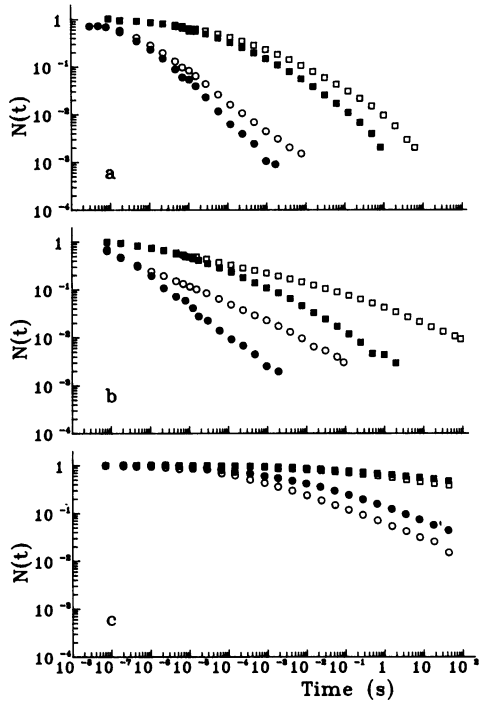

FIGURE 2 Time courses for CO recombination to isolated α^{SH} (*a*) and β^{SH} (*b*) Hb subunits and to SW-Mb (*c*) after photolysis at 60 K (□) and 100 K (○). Open symbols refer to 65% glycerol, solid symbols to 65% ethylene glycol. More details on solvent composition are given in Table 1.

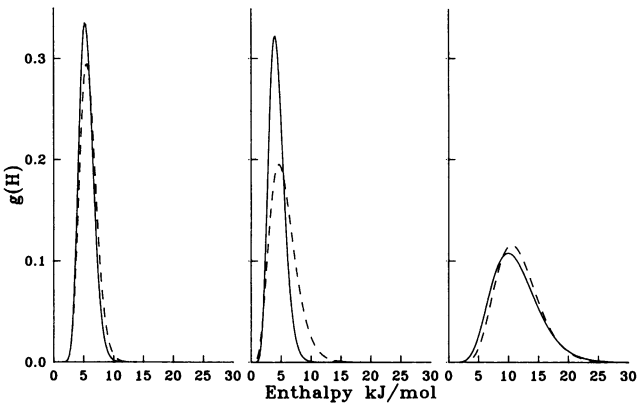

FIGURE 3 Enthalpy distributions for carbon monoxide binding to the isolated α^{SH} (*left*) and β^{SH} (*center*) subunits from HbA and to SW-Mb (*right*) as obtained from flash photolysis measurements between 40 and 110 K in 65% ethylene glycol (*solid lines*) and 65% glycerol (*dashed lines*). The distributions are normalized to unit area. More details on solvent composition are given in Table 1.

the fitting procedures, compared with those obtained when they are forced to assume the same values, are not significantly different. The two kinetic components are therefore distinguishable solely by their preexponential factors both in the α^{SH} and β^{SH} subunits.

For the α^{SH} chains and SW-Mb the solvent effects on the center and width of the enthalpy distribution are barely above the experimental error. In contrast, in the case of the β^{SH} subunits the distribution in glycerol has a somewhat larger H_{peak} and is definitely broader compared with that in ethylene glycol. Fig. 3 also shows that the $g(H)$ profiles are narrowest for the α^{SH}, broader for the β^{SH} chains, and even more so for SW-Mb, in agreement with previously published data (Alberding et al., 1978; Winterhalter and Di Iorio, 1987). Concerning the preexponential factors we note that they are solvent independent only for the α^{SH} chains and that in the other cases are larger for the measurements in glycerol than in ethylene glycol (Table 1).

Fig. 4 shows the visible spectra at various temperatures of the carbonyl derivative of α^{SH} and β^{SH} chains in both solvents used. All spectra consist of two main bands assigned to a single $\pi \rightarrow \pi^*$ transition (Eaton et al., 1978; Eaton and Hofrichter, 1981), the high frequency one (Q_v) being considered the vibronic of that at lower frequency (Q_0). The thermal behavior of the band profiles for the α^{SH} chains is very similar to that reported for human Hb (Cordone et al., 1986) and is practically identical in ethylene glycol/water and in glycerol/water. Instead, sizable differences are found for β^{SH} chains in the two solvents. To obtain the moments of these bands, we have carried out a deconvolution of the spectra in

TABLE 2 The kinetics of CO recombination to the isolated Hb subunits have been fitted using a sum of two processes (Eqs. 4–7) differing only in their pre-exponential k_0 (see also Table 1)

	40 K	50 K	60 K	70 K	80 K	90 K	100 K	110 K
α GL	1.000	0.859	0.861	0.872	0.927	0.946	0.966	0.976
α EG	0.972	0.844	0.848	0.861	0.908	0.944	0.950	0.977
β GL	1.000	0.926	0.922	0.939	0.953	0.960	0.966	0.973
β EG	0.799	0.802	0.882	0.914	0.940	0.962	0.978	0.983

Here we report the fraction of the faster component (f in Eq. 5) obtained from the global fittings of the kinetic traces between 40 and 110 K. More details are given in the data analysis and results sections as well as in part *d* of the discussion. EG = Ethylene glycol; GL = Glycerol.

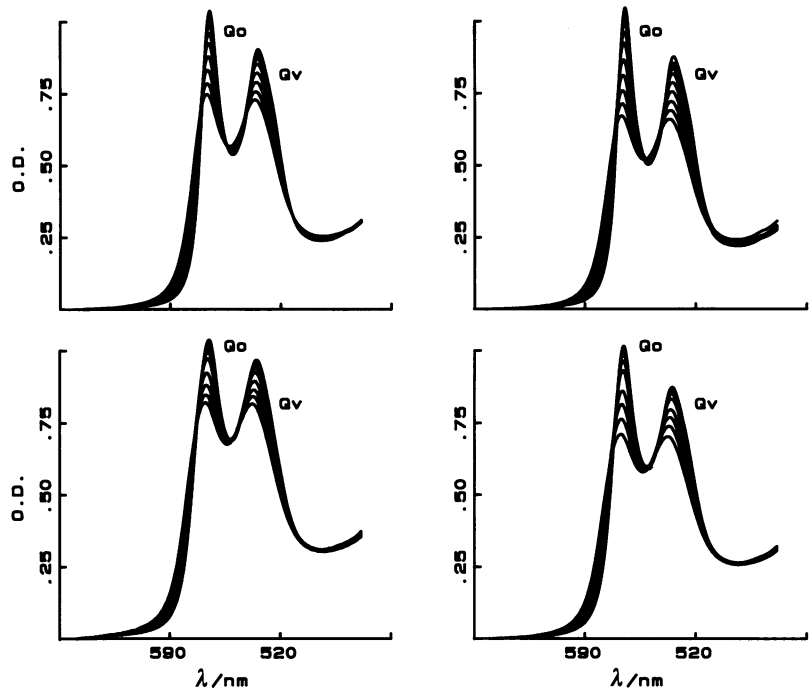

FIGURE 4 Visible absorption spectra of α^{SH}-CO (*top*) and β^{SH}-CO chains (*bottom*) isolated from human Hb. Temperatures range between 20 and 300 K. Left and right panels refer, respectively, to measurements in 65% glycerol and 65% ethylene glycol. More details on solvent composition are given in Table 1.

gaussian components as previously reported for Hb-CO and Mb-CO (Cordone et al., 1988; Leone et al., 1987); two typical deconvolutions are depicted in Fig. 5.

For all proteins lowering the temperature produces an increase of M_0 by $\sim$15% over the temperature range investigated (data not shown) consistent with the thermal contraction of the sample and with a small temperature dependent mixing of the porphyrin π with the iron d orbitals (Cordone et al., 1986; Leone et al., 1987).

In Figs. 6 and 7 the M_1 and M_2 values, relative to the α^{SH}-CO and β^{SH}-CO visible bands Q_0 and Q_v, are reported as a function of temperature along with analogous data on HbA-CO and SW-Mb-CO from the literature (Cordone et al., 1988). The behavior of the α^{SH}-CO chains compares very well with that of Hb-CO; for both proteins M_1 and M_2 are virtually solvent independent at all temperatures and the experimental data can be well fitted by Eqs. 2, giving the results reported in Table 3. For the β^{SH}-CO chains, however, both M_1 and M_2 depend on the solvent composition and the temperature dependence of M_1 displays a barely detectable sigmoidal shape, qualitatively analogous to that reported for SW-Mb. Among all proteins investigated, only for the β^{SH}-CO chains is the second moment of the visible bands influenced by the external medium. The parameters obtained by fitting the thermal behavior of M_1 and M_2 relative to the β^{SH} chains are also given in Table 3.

DISCUSSION

The data shown in Figs. 2, 3, 6, and 7, in Tables 1 and 3 reveal unique optical and kinetic properties for each of the proteins investigated, also in terms of their susceptibility to changes in the solvent composition. Whenever an influence of the external medium on a given protein is seen, this applies to both flash photolysis and absorption spectroscopy data. The most relevant aspects of these results demand a detailed discussion.

a) Differences between proteins

Even without considering solvent effects, the low temperature flash photolysis data reveal characteristic features for each of the proteins investigated, in terms of activation enthalpy distributions $g(H)$ and of preexponential factors k_0 (Fig. 3 and Table 1). Also, the optical spectroscopy data reveal sizable differences among the various proteins in the thermal behavior of M_1 and M_2 of both Q_0 and Q_v (Figs. 6 and 7), resulting in different values of the parameters A, C, and D (Table 3).

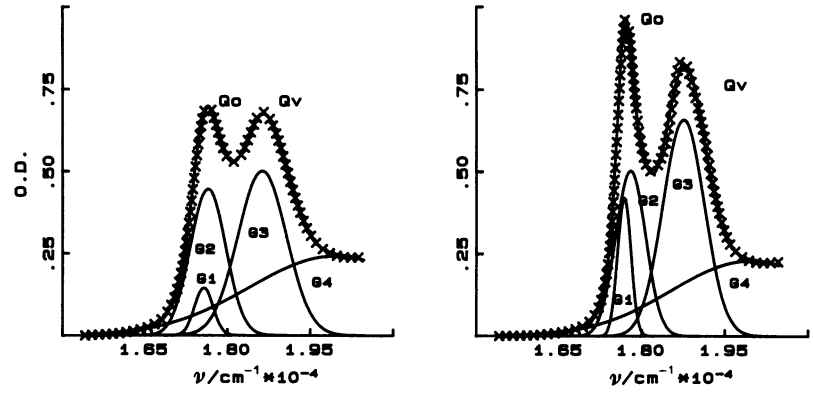

FIGURE 5 Deconvolution of the visible spectra of α^{SH}-CO chains in terms of gaussian components. (*Left*) $T = 298$ K, (*right*) $T = 20$ K; both spectra are in 65% glycerol. Dots are the experimental points; the continuous lines represent the gaussian components and the synthesized band profile. For the sake of clarity not all the experimental points are included. Following the procedure described under methods, we have deconvoluted the spectra using two gaussians (G_1 and G_2) for Q_0, one (G_3) for Q_v, and G_4 as background. Mean square deviations are $1.9 \cdot 10^{-3}$ at $T = 298$ K and $1.0 \cdot 10^{-3}$ at $T = 20$ K.

b) Solvent effects

Changes in the solvent composition influence differently the kinetic and optical spectroscopy properties of each of the proteins investigated. For the sake of clarity we analyze them individually.

i) α^{SH} chains

The $g(H)$ distributions and the preexponential factors for low temperature CO recombination to the α chains (Fig. 3 *a* and Table 1), as well as the thermal evolution of the optical spectra (Figs. 6 and 7 and Table 3), can be regarded as solvent independent. Very tiny differences between the M_1 and M_2 values of both Q_0 and Q_v bands in the two solvents are detected only in the low temperature range and parallel the minimal differences between the $g(H)$ distributions in ethylene glycol/water and in glycerol/water.

ii) β^{SH} chains

The low temperature CO rebinding kinetics to the β hemoglobin subunits are faster in ethylene glycol/water than in glycerol/water (Fig. 2 *b*). Opposite enthalpic and entropic effects (Fig. 3 *b* and Table 1) contribute to the determination of the reaction velocity and partially compensate each other. In fact, the $g(H)$ distribution in glycerol/water is broader and slightly displaced toward higher enthalpies with respect to that in ethylene glycol/water whereas the log (k_0) values are larger in glycerol than in ethylene glycol. The spectroscopic data display solvent-dependent thermal evolutions of M_1 and M_2 for both Q_0 and Q_v (Figs. 6 and 7) and the results of the fittings to Eqs. 2 yield larger C and smaller D values in glycerol/water than in ethylene glycol/water.

iii) Sperm whale myoglobin

Also in this case the solvent composition influences the time course for CO rebinding, but, compared with the β chains, produces opposite effects being CO rebinding faster in glycerol than in ethylene glycol (Fig. 2 *c*). This result is in agreement with a previous report by Cordone et al. (1990) and reflects large differences in the preexponential factor and minor ones in the $g(H)$ distributions (Fig. 3 *c* and Table 1). The different kinetic behavior of SW-Mb in the two solvents can thus be ascribed mainly to an entropic effect.

Concerning the spectroscopic data, the results depicted in Figs. 6 and 7 and in Table 3 show that the M_2 thermal behavior for both visible bands is, in SW-Mb, unaffected by the solvent composition. In contrast, the temperature dependence of M_1 is influenced by the solvent and exhibits a marked sigmoidal shape. Furthermore, at low temperatures the values of M_1 are higher in ethylene glycol than in glycerol (Fig. 6).

c) Correlation between kinetic and spectroscopic behavior

A relevant point, emerging from this investigation, is the correlation between the solvent effects in the CO binding kinetics and on the thermal evolution of the optical absorption spectra.

The first correlation is between the width of the $g(H)$ distributions (Fig. 3) and the values of the parameter C in Table 3. Broad enthalpy distributions correspond to large C values and, as the $g(H)$ becomes narrower, the parameter C drops down to nearly zero, as for the Q_0 band of the α chains (Table 3). This correlation holds for

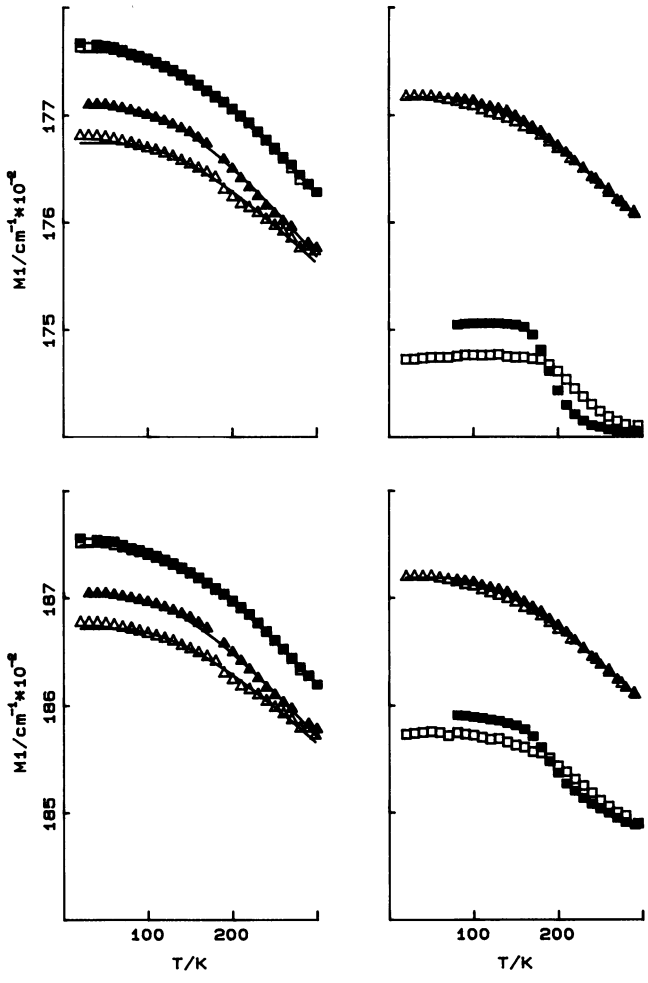

FIGURE 6 Temperature dependence of M_1 for Q_0 (*top*) and Q_v (*bottom*) bands of α^{SH}-CO (□) and β^{SH}-CO chains (△) (*left*), and of Hb-CO (△) and SW-Mb-CO (□) (*right*). Open symbols correspond to data obtained in 65% glycerol, solid symbols in 65% ethylene glycol. The solid lines represent the fit to the experimental values obtained using Eq. 2*a*. In the case of myoglobin the fittings could not be performed.

all proteins investigated, in both solvents and for both spectral bands (Q_0 and Q_v). When $g(H)$ is solvent independent (α chains and SW-Mb) M_2 and C are not influenced by the external medium. Conversely, when the width of the $g(H)$ distribution depends on the solvent composition, as for the β subunits, M_2 and C are also affected.

As pointed out in the theoretical section, C takes into account *i*) the homogeneous broadening of the spectral bands, *ii*) the coupling of the electronic transition with high frequency modes, and *iii*) inhomogeneous line broadening due to the presence of substates. The high frequency modes-coupling[2] and/or the homogeneous line broadening of the spectral bands are likely to be fairly insensitive to changes in the external medium and therefore we ascribe the solvent effect on parameter C, observed for the β chains (Table 3), to differences in the distribution of conformational substates. Taking into account the effect of the external medium on the $g(H)$ distributions relative to the β chains (Fig. 3 *b*), this interpretation of the solvent dependence of C implies a nonrandom mapping between the frequency of the optical transitions and the enthalpy barrier for CO rebinding from inside the heme pocket. The difference between the C values obtained for the Q_0 band of the β chains in the two solvents (~ 70 cm^{-1}) gives an estimate of the contribution of the inhomogeneous broadening to the width of the optical bands. More quantitative conclusions cannot be drawn from our data due to the high standard deviations in the estimated values of the fitting parameters (Table 3). The presence of inhomogeneous broadening in the spectral bands of SW-Mb and the correlation between spectral and functional heterogeneity has been already proposed to explain the blue shift of the Mb-CO Soret, Mb near IR (~ 760 nm), and IR CO stretching bands occurring during carbon monoxide rebinding after photolysis (Ansari et al., 1987; Ansari, 1988; Ormos et al., 1990).

A further correlation, between the values of the preexponential factor and those of M_1 at low temperatures, emerges from the data reported in Table 1 and in Fig. 6. Whenever the solvent composition influences log (k_0) (β chains and SW-Mb), a change of M_1 is also observed in the opposite direction. Some considerations can be made on the possible physical origin of this correlation. The preexponential factor k_0 contains the entropic contribution to the free energy of ligand binding and has been related to the effective volume of the heme pocket (Braunstein et al., 1988; Frauenfelder and Wolynes, 1985). One would therefore expect an increase in k_0 if the constraints imposed by the external medium on the protein produce a decrease in the volume of the heme pocket. The distal residues E7 and E11 have already been proposed as responsible, to a large extent, for the changes in the heme-pocket free volume (Braunstein et al., 1988) and the "packing" of the heme cavity is likely to influence the geometry assumed by the bound CO. Thus, in SW-Mb the most populated of the three different geometries of bound CO (A states), detected both by IR spectroscopy (Ormos et al., 1988) and x-ray

[2]We note that these high frequency modes occur most likely within the heme plane (heme macrocyclic vibrations) and their frequency and coupling to the $\pi \rightarrow \pi^*$ transitions should be fairly insensitive to the average protein structure.

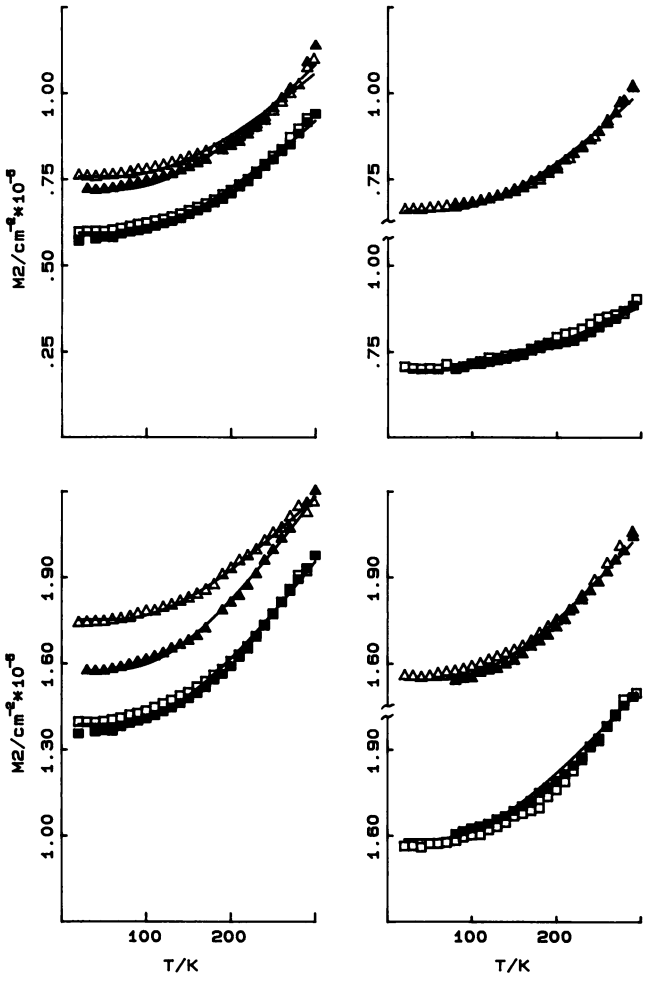

FIGURE 7 M_2 values as function of temperature for Q_0 (*top*) and Q_v (*bottom*) bands of α^{SH}-CO (□) and β^{SH}-CO chains (Δ) (*left*), and of Hb-CO (△) and SW-Mb-CO (□) (*right*). Open symbols refer to 65% glycerol, solid symbols to 65% ethylene glycol. The continuous lines represent the fit to the experimental values obtained using Eq. 2*b*.

crystallography (Kuriyan et al., 1986), is "off-axis" by ~28° (Braunstein et al., 1988) while in the synthetic SW-Mb mutant, in which the distal histidine is replaced by a glycine with a considerable increase of heme-pocket volume, only one IR CO stretching band is seen, corresponding to a geometry of binding which deviates by 20° from the heme normal (Braunstein et al., 1988). The log (k_0) values for low temperature CO binding in glycerol/water to native SW-Mb and to its mutant with the distal glycine are, respectively, 9 and 8.4 (Table 1; Braunstein et al., 1988). On the basis of these observations it could be proposed that to a displacement of the distal residues away from the heme should correspond an increase in the heme pocket free volume and, as a consequence, a more axial geometry of CO binding and a decrease in k_0. If the dipolar nature of the CO molecule is taken into account one can predict a reduction of the component of the dipole moment perpendicular to the heme plane upon tilting of the bound CO away from the axial configuration. This in turn, on the basis of simple electrostatic considerations, is expected to lower the ΔE relative to the in plane-polarized $\pi \rightarrow \pi^*$ transition and therefore the low temperature M_1 values of the visible bands. An increase in the off-axis geometry of CO binding should thus result in a red shift of the visible bands and, conversely, a blue shift would be indicative of a more axial binding geometry. The above arguments rationalize, to a first approximation, the inverse relationship between the solvent effects on the low temperature M_1 values and on k_0 found for the β chains and SW-Mb (Fig. 6, Tables 1 and 3) and the absence of solvent effects on M_1 and k_0 in the α chains (Fig. 6 and Table 1). Nevertheless, the absolute values of M_1 and k_0 relative to this protein indicate a more complex situation. In fact, at low temperatures M_1 for the α chains is higher than for any other of the proteins investigated in this work, thus implying a more axial geometry of CO binding. This agrees with *i*) the position of the single IR CO stretching band, centered at ~1,955 cm^{-1} (D. Braunstein and S. Luck, personal communication), compared with 1,945 cm^{-1} measured for the major "A state" in SW-Mb (Braunstein et al., 1988), *ii*) with x-ray crystallography results showing a reduced steric hindrance at the distal side of the α subunit within the Hb tetramer (Perutz et al., 1987), and *iii*) with XANES data indicating a more linear geometry for the Fe-CO bond in the α chains than in the β or in SW-Mb (Congiu Castellano et al., 1989). But the values of k_0 for CO binding to the α chains, if compared with those relative to SW-Mb, are apparently inconsistent with a larger effective volume of the heme pocket in the former protein. This inconsistency implies the existence of other factors, which can vary considerably in different proteins, in determining k_0, e.g. the ratio between the number of unbound and activated states that the ligand can populate or the contribution from the whole protein to the entropy of ligation.

d) Heterogeneity of the low T kinetics time courses

The low temperature kinetics for CO recombination to the isolated Hb subunits cannot be well approximated by a single $g(H)$ distribution (Eqs. 3 and 4). Instead, good fittings (e.g. Fig. 1) are obtained using the double distribution model described in Data Analysis (Eq. 5). Although this is not a major aspect of the investigation

TABLE 3 **Values of the parameters obtained by fitting Eqs. 2 to the temperature dependence of M_1 and M_2 determined for Q_0 and Q_v bands of the carbonyl α^{SH} and β^{SH} subunits from human Hb**

	A	ν	C	D	F
	$cm^{-1} \cdot 10^{-4}$	cm^{-1}	$cm^{-1} \cdot 10^{-2}$	$cm^{-1} \cdot 10^{-4}$	$cm^{-1} \cdot 10^{-2}$
α (Qo band)	5.9 ± 0.6	325 ± 25	0.0 ± 0.01	1.800 ± 0.002	−2.4 ± 0.2
β GL (Qo band)	5.4 ± 1.0	325 ± 25	1.5 ± 0.30	1.788 ± 0.002	−2.1 ± 0.3
β EG (Qo band)	6.5 ± 1.5	325 ± 25	0.8 ± 0.30	1.796 ± 0.002	−2.4 ± 0.2
Hb (Q_0 band)	6.2 ± 1.2	325 ± 15	0.7 ± 0.80	1.79 ± 0.002	−2.0 ± 0.2
Mb (Qo band)	2.6 ± 0.4	285 ± 20	2.1 ± 0.90	—	—
α (Qv band)	10.2 ± 0.9	320 ± 15	1.9 ± 0.20	1.898 ± 0.002	−2.3 ± 0.2
β GL (Qv band)	7.7 ± 0.7	325 ± 15	3.1 ± 1.00	1.887 ± 0.002	−2.0 ± 0.2
β EG (Qv band)	10.9 ± 0.9	325 ± 15	2.2 ± 0.20	1.894 ± 0.002	−2.3 ± 0.2
Hb (Qv-band)	9.1 ± 1.0	325 ± 15	2.5 ± 0.20	1.892 ± 0.002	−2.0 ± 0.2
Mb (Qv band)	7.4 ± 0.9	285 ± 20	2.9 ± 0.20	—	—

Analogous data obtained for Hb and SW-Mb (Cordone et al., 1988) are also given for comparison. No values for the parameters D and F are reported for SW-Mb in view of the sigmoidal behavior of its M_1 temperature dependence. See Table 1 for details on solvent composition. EG = Ethylene glycol; GL = Glycerol.

reported in this paper, it deserves some comments. We propose, to tentatively interpret the phenomenon, a correlation between the kinetic heterogeneity and the multiplicity of states which the bound and the photolyzed CO molecule can populate, that is the A and B states according to the terminology adopted by the Frauenfelder group (Alben et al., 1982). The low temperature FTIR spectra of the isolated α chains display a single CO stretching band when the ligand is bound to the heme-iron and two when it is photolyzed (D. Braunstein, unpublished results), a situation which could lead to biphasic flash photolysis time courses. For SW-Mb the number of A and B states is too high (Ansari et al., 1987) to be detected in our kinetic measurements and therefore the experimental traces can be fitted with a single enthalpy distribution. Unfortunately, the data presently available are not sufficient to provide a solid explanation of the observed kinetic behavior.

e) M_1 temperature dependence

Finally, we would like to comment on the interpretation given in a previous investigation (Cordone et al., 1988) for the sigmoidal behavior of the M_1 temperature dependence in SW-Mb, as compared with the smooth thermal evolution of M_1 in Hb. This finding had been attributed to the different state of aggregation or to a different compressibility of the two proteins. The data reported here rule out the first interpretation, but are consistent with the second. The fact that the M_1 thermal evolution in Hb is not the average of those of the isolated subunits and is solvent independent (Fig. 6) can also be explained in terms of differences in compressibility between the subunits. Thus, in keeping with their narrow and solvent independent $g(H)$ distributions, as compared with those of β chains (Fig. 3 and Table 1), the α chains are capable to buffer the constraints imposed by the external medium on the Hb tetramer.

CONCLUSIONS

The picture that we propose on the basis of our results is the following: I) The α chains, with their solvent-independent narrow $g(H)$ distributions (Fig. 3 *a*) and low C values (Table 3) display the lowest functional and spectroscopic heterogeneity and have a low level of steric hindrance at the distal side of the heme. This situation is consistent with a small distal contribution to the enthalpy of ligand binding.

II) The β chains have a larger heterogeneity than the α subunits, both in kinetic (Fig. 3 *b* and Table 1) and spectroscopic (Table 3 and Fig. 7) terms. Futhermore the solvent composition influences the shape and position of the $g(H)$ distributions as well as M_2. The low temperature M_1 values and the log (k_0) are indicative of a higher packing of the heme pocket and a CO geometry of binding slightly more tilted as compared with the α chains. The difference with the α chains is larger in glycerol than in ethylene glycol. The postulated increase of distal side hindrance, combined with the fairly small H_{peak} values shown in Fig. 3 *b*, renders the overall enthalpy of CO binding to the β chains sensitive to changes in the solvent composition.

III) Sperm whale Mb exhibits, among the proteins investigated, the largest structural and functional heterogeneity. The peak enthalpy for CO rebinding from inside the heme-pocket is considerably larger than in the Hb subunits (~10 kJ · M^{-1} vs. 4–5.5 kJ · M^{-1}) and the packing of the heme-pocket is higher. Under these conditions, the structural perturbations induced by

changes in the solvent composition (mainly of distal nature) cannot significantly contribute to the overall enthalpy of ligand binding. This explains why in SW-Mb the $g(H)$ distribution is practically unaffected by the solvent, even though some alteration at the distal side of the heme are likely to occur, as shown by the changes in the low temperature M_1 (Fig. 6) and in the preexponential values (Table 1).

The authors wish to thank H. Frauenfelder and his group for helpful discussions and for providing us, prior to publication, the work by Ormos et al. (1990). The technical help by J. Forrer, V. Greco, W. Jäggi, G. Lapis, A. Lehman, P. Nyffeler, and M. Quartararo is highly appreciated. We would particularly like to thank Joel Berendzen and Todd B. Sauke for having built for us the logarithmic data averaging transient recorder (Wondertoy II).

This work has been supported by the Swiss National Science Foundation grants 3.123–0.85 and 31.9423.88, by the ETH special credit 03586/41–1080.5 (Dr. Di Iorio, Dr. Hiltpold, Dr. Filipovic, and Dr. Winterhalter), by the National Institutes of Health grant RR03155 (Dr. Gratton), and by the "Ministero della Pubblica Istruzione" (Dr. Vitrano, Dr. Cupane, Dr. Leone, Dr. Cordone). General indirect support from CRRNSM to Dr. Vitrano, Dr. Cupane, Dr. Leone, and Dr. Cordone is also acknowledged.

Received for publication 9 May 1990 and in final form 13 September 1990.

REFERENCES

Alben, J. O., D. Beece, S. F. Bowne, W. Doster, L. Eisenstein, H. Frauenfelder, D. Good, J. D. McDonald, M. C. Marden, P. P. Moh, L. Reinisch, A. H. Reynolds, E. Shiamsunder, and K. T. Yue. 1982. Infrared spectroscopy of photodissociated carboxy-myoglobin at low temperatures. *Proc. Natl. Acad. Sci. USA.* 79:3744–3748.

Alberding, N., S. C. Shirley, L. Eisenstein, H. Frauenfelder, D. Good, I. C. Gunsalus, T. M. Nordlund, M. F. Perutz, A. H. Reynolds, and L. B. Sorensen. 1978. Binding of carbon monoxide to isolated hemoglobin chains. *Biochemistry.* 17:43–51.

Ansari, A. 1988. Conformational relaxation and kinetic hole-burning in Sperm whale myoglobin. Ph.D. thesis. University of Illinois at Urbana-Champaign. 84

Ansari, A., E. E. Di Iorio, D. D. Dlott, H. Frauenfelder, I. E. T. Iben, P. Langer, H. Roder, T. B. Sauke, and E. Shyamsunder. 1986. Ligand binding to heme proteins: relevance of low-temperature data. *Biochemistry.* 25:3139–3146.

Ansari, A., J. Berendzen, D. Braunstein, B. R. Cowen, H. Frauenfelder, M. K. Hong, I. E. T. Iben, J. B. Johnson, P. Ormos, T. B. Sauke, R. Scholl, A. Schulte, P. J. Steinbach, J. Vittitov, and R. D. Young. 1987. Rebinding and relaxation in the myoglobin pocket. *Biophys. Chem.* 26:337–355.

Austin, R. H., K. W. Beeson, L. Eisenstein, H. Frauenfelder, and I. C. Gunsalus. 1975. Dynamics of ligand binding to myoglobin. *Biochemistry.* 14:5355–5373.

Baldini, G., E. Mulazzi, and N. Terzi. 1965. Isotope effects induced by local modes in the U Band. *Physiol. Rev.* 140:2094–2101.

Beechem, J. M., and E. Gratton. 1988. Fluorescence spectroscopy data analysis environment: a second generation Global analysis program. *SPIE (Society of Photo-Optical Instrumentation Engineers).* 909:70–81.

Bevington, P. R. 1969. Data Reduction and Error Analysis for the Physical Sciences. McGraw-Hill Book Co., New York. 336 pp.

Braunstein, D. 1991. pH Effects and rebinding pathways in CO adducts of heme proteins. Ph.D. thesis. University of Illinois at Urbana-Champaign. In press.

Braunstein, D., A. Ansari, J. Berendzen, B. R. Cowen, K. D. Egeberg, H. Frauenfelder, M. K. Hong, P. Ormos, T. B. Sauke, R. Scholl, A. Schulte, S. G. Sligar, B. A. Springer, P. J. Steinbach, and R. D. Young. 1988. Ligand binding to synthetic mutant myoglobin (His-E7 → Gly): role of the distal histidine. *Proc. Natl. Acad. Sci. USA.* 85:8497–8501.

Bucci, E. 1981. Preparation of isolated chains of human hemoglobin. *Methods Enzymol.* 76:97–106.

Congiu Castellano, A., M. Castagnola, E. Burattini, M. Dell'Ariccia, S. Della Longa, A. Giovannelli, P. J. Durham, and A. Bianconi. 1989. Heterogeneity of the isolated subunits of the fetal and adult human hemoglobin in solution, detected by XANES spectroscopy. *Biochem. Biophys. Acta.* 996:240–246.

Cordone, L., A. Cupane, M. Leone, and E. Vitrano. 1986. Optical absorption spectra of deoxy- and oxyhemoglobin in the temperature range 300-20 K. Relation with protein dynamics. *Biophys. Chem.* 24:259–275.

Cordone, L., A. Cupane, M. Leone, E. Vitrano, and D. Bulone. 1988. Interaction between external medium and heme pocket in myoglobin probed by low temperature optical spectroscopy. *J. Mol. Biol.* 199:213–218.

Cordone, L., A. Cupane, M. Leone, and E. Vitrano. 1990. Thermal behavior of the 760 nm absorption band in photodissociated sperm whale myoglobin at cryogenic temperatures: dependence on external medium. *Biopolymers.* 29:639–643.

Cupane, A., M. Leone, E. Vitrano, and L. Cordone. 1988. Structural and dynamic properties of the heme pocket in myoglobin probed by optical spectroscopy. *Biopolymers.* 27:1977–1997.

Dexter, D. L. 1958. Theory of the optical properties of imperfections in nonmetals. *In* Solid State Physics. F. Seitz and D. Turnbull, editors. Academic Press, New York. 353–411.

Dlott, D. D., H. Frauenfelder, P. Langer, H. Roder, and E. E. Di Iorio. 1983. Nanosecond flash photolysis study of carbon monoxide binding to the beta chains of hemoglobin Zurich [β_{63} (E7) His → Arg]. *Proc. Natl. Acad. Sci. USA.* 80:6239–6243.

Doster, W., D. Beece, S. F. Bowne, E. E. Di Iorio, L. Eisenstein, H. Frauenfelder, L. Reinisch, E. Shyamsunder, K. H. Winterhalter, and K. T. Yue. 1982. Control and pH dependence of ligand binding to heme proteins. *Biochemistry.* 21:4831–4839.

Eaton, W. A., and J. Hofrichter. 1981. Polarized absorption and linear dichroism spectroscopy of hemoglobin. *Methods Enzymol.* 76:175–261.

Eaton, W. A., L. K. Hanson, P. J. Stephens, J. C. Sutherland, and J. B. R. Dunn. 1978. Optical spectra of oxy- and deoxyhemoglobin. *J. Am. Chem. Soc.* 100:4991–5003.

Frauenfelder, H., and P. G. Wolynes. 1985. Rate theories and puzzles of hemeprotein kinetics. *Science (Wash. DC).* 229:337–345.

Geraci, G., L. J. Parkhurst, and Q. H. Gibson. 1969. Preparation and properties of α- and β-chains from human hemoglobin. *J. Biol. Chem.* 244:4664–4667.

Ikeda-Saito, M., T. Inubushi, and T. Yonetani. 1981. Preparation of hybrid hemoglobins with different prostetic groups. *Methods Enzymol.* 76:113–121.

Kuriyan, J., S. Wilz, M. Karplus, and G. A. Petsko. 1986. X-Ray structure and refinement of carbon monoxy (iron II)-myoglobin at 1.5 Angstrom resolution. *J. Mol. Biol.* 192:133–154.

Leone, M., A. Cupane, E. Vitrano, and L. Cordone. 1987. Dynamic properties of oxy- and carbonmonoxyhemoglobin probed by optical spectroscopy in the temperature range 300–200 K. *Biopolymers.* 26:1769–1779.

Markham, J. J. 1959. Interactions of normal modes with electron traps. *Rev. Mod. Phys.* 31:956–989.

Marquardt, D. W. 1963. An algorithm for least-squares estimation of nonlinear parameters. *J. Soc. Ind. Appl. Math.* 11:431–441.

Ormos, P., D. Braunstein, H. Frauenfelder, M. K. Hong, S. L. Lin, T. B. Sauke, and R. D. Young. 1988. Orientation of carbon monoxide and structure-function relationship in carbonmonoxymyoglobin. *Proc. Natl. Acad. Sci. USA.* 85:8492–8496.

Ormos, P., A. Ansari, D. Braunstein, B. R. Cowen, H. Frauenfelder, M. K. Hong, I. E. T. Iben, T. B. Sauke, P. Steinbach, and R. D. Young. 1990. Inhomogeneous broadening in spectral bands of carbonmonoxymyoglobin: the connection between spectral and functional heterogeneity. *Biophys. J.* 57:191–199.

Perutz, M. F., G. Fermi, B. Luisi, B. Shaanan, and R. C. Liddington. 1987. Stereochemistry of cooperative mechanisms in hemoglobin. *Biochemistry.* 20:309–321.

Schomacker, K. T., and P. M. Champion. 1986. Investigations of spectral broadening mechanisms in biomolecules: cytochrome C. *J. Chem. Phys.* 84:5314–5325.

Srajer, V., K. T. Schomacker, and P. M. Champion. 1986. Spectral broadening in biomolecules. *Phys. Rev. Lett.* 57:1267–1270.

Srajer, V., L. Reinisch, and P. M. Champion. 1988. Protein fluctuations, distributed coupling, and the binding of ligands to heme proteins. *J. Am. Chem. Soc.* 110:6656–6670.

Winterhalter, K. H., and A. Colosimo. 1971. Chromatographic isolation and characterization of isolated chains from hemoglobin after regeneration of sulphydryl groups. *Biochemistry.* 10:621–624.

Winterhalter, K. H., and E. E. Di Iorio. 1987. Deformability of the hemoglobin molecule as the basis of its functional behavior. *Acta Haematol. (Basel).* 78:90–94.

Young, R. D., and S. F. Bowne. 1984. Conformational substates and barrier height distributions in ligand binding to heme proteins. *J. Chem. Phys.* 81:3730–3737.